Australian Journal of Mechanical Engineering

ISSN: 1448-4846 (Print) 2204-2253 (Online) Journal homepage: https://engineersaustralia.tandfonline.com/loi/tmec20

Thermal and structural analysis of disc brake assembly during single stop braking event

Ali Belhocine, Abd Rahim Abu Bakar & Mostefa Bouchetara

To cite this article: Ali Belhocine, Abd Rahim Abu Bakar & Mostefa Bouchetara (2016) Thermal and structural analysis of disc brake assembly during single stop braking event, Australian Journal of Mechanical Engineering, 14:1, 26-38, DOI: 10.1080/14484846.2015.1093213

To link to this article: https://doi.org/10.1080/14484846.2015.1093213

AUSTRALIAN JOURNAL OF MECHANICAL ENGINEERING, 2016
VOL. 14, NO. 1, 26–38
http://dx.doi.org/10.1080/14484846.2015.1093213

Taylor & Francis
Taylor & Francis Group

Thermal and structural analysis of disc brake assembly during single stop braking event

Ali Belhocine[a], Abd Rahim Abu Bakar[b] and Mostefa Bouchetara[a]

[a]Faculty of Mechanical Engineering, University of Sciences and the Technology of Oran, 31000 Oran, Algeria; [b]Faculty of Mechanical Engineering, Department of Automotive Engineering, Universiti Teknologi Malaysia, 81310, Skudai, Malaysia

ABSTRACT

An automobile disc brake system is used to perform three basic functions, i.e. to reduce speed of a vehicle, to maintain its speed when travelling downhill and to completely stop the vehicle. During these braking events, the disc brake may suffer from structural and wear issues. It is quite sometimes that the disc brake components fail structurally and/or having severe wear on the pad. Thus, this paper aims to determine disc temperature and to examine stress concentration, structural deformation and contact pressure of brake disc and pads during single braking stop event by employing commercial finite-element software, ANSYS. The paper also highlights the effects of using a fixed calliper, different friction coefficients and different speeds of the disc on the stress concentration, structural deformation and contact pressure of brake disc and pads, respectively. The thermal-structural analysis is then used with coupling to determine the deformation and the Von Mises stress established in the disc, the contact pressure distribution in pads.

ARTICLE HISTORY
Received 26 November 2013
Accepted 5 May 2014

KEYWORDS
Disc brake; Von Mises stress; structural deformation; contact pressure; finite element

1. Introduction

Passenger car disc brakes are safety-critical components whose performance depends strongly on the contact conditions at the pad to rotor interface. When the driver steps on the brake pedal, hydraulic fluid is pushed against the piston, which in turn forces the brake pads into contact with the rotor. The frictional forces at the sliding interfaces between the pads and the rotor retard the rotational movement of the rotor and the axle on which it is mounted (Söderberg and Andersson 2009). The kinetic energy of the vehicle is transformed into heat that is mainly absorbed by the rotor and the brake pad.

The frictional heat generated on the interface of the disc and the pads can cause high temperature. Particularly, the temperature may exceed the critical value for a given material, which leads to undesirable effects, such as brake fade, local scoring, thermoelastic instability, premature wear, brake fluid vaporization, bearing failure, thermal cracks and thermally excited vibration as referred to (Lee and Yeo 2000; Gao and Lin 2002). Gao and Lin (2002) stated that there was considerable evidence to show that the contact temperature is an integral factor reflecting the specific power friction influence of combined effect of load, speed, friction coefficient, and the thermo physical and durability properties of the materials of a frictional couple. Lee and Yeo (2000) reported that uneven distribution of temperature at the surfaces of the disc and friction pads brings about thermal distortion, which is known as coning and found to be the main cause of judder and disc thickness variation. Abu Bakar, Ouyang, and Li (2009) in their recent work found that temperature could also affect vibration level in a disc brake assembly. Valvano and Lee (2000) simulated thermal analysis on a disc brake with a combination of computer-based thermal model and finite-element (FE)-based techniques to provide a reliable method to calculate the temperature rise, thermal stress and distortion under a given brake schedule. Wolejsza et al. (2001) performed analysis on the thermo-mechanical behaviour of airplane carbon composite brakes using MSC/Marc FE software which allows accurate simulation of the transient heat transfer phenomenon coupled to disc deformations caused by frictional sliding contact.

There are three types of mechanical stresses subjected by the disc brake. The first one is the traction force created by the centrifugal effect due to the rotation of the disc brake when the wheel is rotating and no braking force is applied to the disc. During braking operation, there are another two additional forces experienced by

CONTACT Ali Belhocine al.belhocine@yahoo.fr

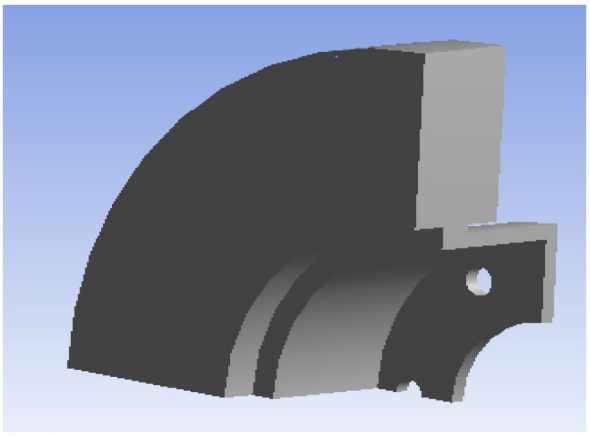

Figure 1. Full disc.

the disc brake. Firstly, compression force is created as the result of the force exerted by the brake pad pressing perpendicular onto the surface of the disc to slow it down. Secondly, the braking action due to the rubbing of the brake pad against the surface of the disc brake is translated into frictional or traction force on the disc surface which acts in the opposite direction of the disc rotation.

A disc brake of floating caliper design typically consists of pads, calliper, carrier, rotor (disc), piston and guide pins. One of the major requirements of the calliper is to press the pads against the rotor and should ideally achieve as uniform interface pressure as possible. A uniform pressure between the pads and rotor leads to uniform pad wear and brake temperature, and more even friction coefficients as cited in Limpert (1999). Unevenness of the pressure distribution could cause uneven wear and shorter life of pads. It has also speculated that they may promote disc brake squeal. The interface pressure distributions have been investigated by a number of people. Tirovic and Day (1991) studied the influence of component geometry, material properties and contact characteristics on the interface pressure distribution. They used a simple and nonvalidated, three-dimensional model of the disc brake. Tamari, Doi, and Tamasho (2000) presented a method of predicting disc brake pad contact pressure for certain operating condition by means of experimental and numerical methods. They developed a quite detailed model and validated the model by fitting the numerical deformations of the disc brake components with experimental results. Hohmann et al. (1999) also presented a method of contact analysis for the drum and disc brakes of simple three-dimensional models using ADINA software package. They showed a sticking and shifting contact area in their results. Like Tirovic and Day (1991), validation of their model was not made, Ripin (1995) developed a simple, validated three-dimensional FE model of the pad, and applied rather simple piston and finger force onto the back plate interface in his analysis. He studied the contact pressure distribution at the disc/pad interface, where gap elements were used to represent contact effect.

In this paper, thermal and structural analysis is performed on a simple FE model of a real disc brake assembly to obtain the temperature established on the disc, the contact pressure distributions on the friction pads and the Von Mises stress in disc interface by utilizing the ANSYS 11.0 FE software. Sensitivity study on rotation of the disc, load pattern and coefficient of friction is also performed.

2. Heat flux entering the disc

The initial heat flux q_0 into the rotor face is directly calculated using the following formula (Reimpel 1998):

$$q_0 = \frac{1-\phi}{2}\frac{m\,g\,v_0\,z}{2A_d\varepsilon_p} \tag{1}$$

where $z = a/g$ is the braking effectiveness, a is the deceleration of the vehicle [m/s^2], ϕ is the rate distribution of the braking forces between the front and rear axle, A_d disc surface swept by a brake pad [m^2], v_0 is the initial speed of the vehicle [m/s], ε_p is the factor load distribution on the disc surface, m is the mass of the vehicle [kg] and g is the acceleration of gravity (9.81) [m/s^2].

There are two types of disc: full discs and ventilated discs. The full discs, of simple geometry and thus of simple manufacture, are generally placed on the rear axle of the car. They are composed quite simply of a full crown connected to a "bowl" which is fixed on the hub of the car.

The ventilated discs, of more complex geometry, appeared more tardily (Figure 1). They are most of the time on the nose gear. However, they are increasingly at the rear and front cars upscale. Composed of two crowns – called flasks – separated by fins (Figure 2), they cool better than the full discs thanks to ventilation between the fins which, moreover, promote convective heat transfer by increasing the exchange surfaces discs. The ventilated disc comprises more matter than the full disc; its capacity for calorific absorption is thus better.

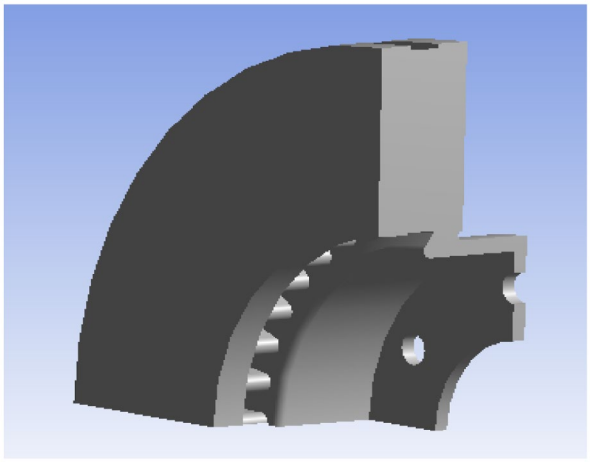

Figure 2. Ventilated disc.

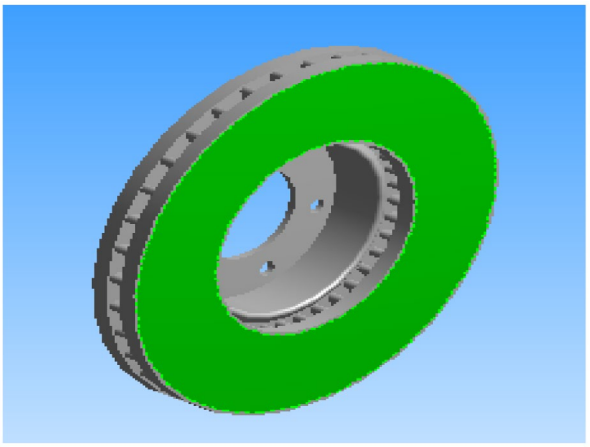

Figure 3. Application of flux.

The brake disc consumes the major part of the heat, usually greater than 90%, by means of the effective contact surface of the friction coupling. Considering the complexity of the problem and the limitation in the average data processing, one identifies the pads by their effect, represented by an entering heat flux (Figure 3).

The loading corresponds to the heat flux on the disc surface. The dimensions and the parameters used in the thermal calculation are recapitulated in Table 1.

The material of brake disc is grey cast iron (GF) with high carbon content, with good thermophysical characteristics, thermoelastic characteristics of which adopted in this simulation of the rotor and the pads are recapitulated in Table 2.

The thermal conductivity and specific heat are a function of temperature (Figures 4 and 5).

3. Modelling in ANSYS CFX

Considering symmetry in the disc, one took only the quarter of the geometry of the fluid field (Figure 6) using software ANSYS ICEM CFD.

This stage consists in preparing the mesh of the fluid field. In our case, one used a linear tetrahedral element with 30,717 nodes and 179,798 elements (Figure 7).

3.1. Results of the calculation of the heat transfer coefficient h

The heat transfer coefficient is a parameter relates with the velocity of air and the shape of brake disc, and many other factors. In different velocity of air, the heat transfer coefficient in different parts of brake disc changes with time. Heat transfer coefficient will depend on air flow in the region of brake rotor and vehicle speed, but it does not depend on material. In this simulation, it is determined the average value of the coefficient *h* "Wall heat Transfer Coefficient", variable with time (Figures 8 and 9).

3.2. Meshing details

The goal of meshing in Workbench is to provide robust, easy to use meshing tools that will simplify the mesh generation process. The model using must be divided into a number of small pieces known as FEs. Since the model is divided into a number of discrete parts, to carry out a FE analysis. A FE mesh model generated is shown in Figure 10. The mesh results are as shown in Table 3. The elements used for the mesh of the model are tetrahedral three-dimensional elements.

Table 1. Input parameters.

Description	Values
Inner disc diameter, mm	66
Outer disc diameter, mm	262
Disc thickness (TH), mm	29
Disc height (H), mm	51
Vehicle mass m, kg	1385
Initial speed v_0, m/s	28
Deceleration a, m/s$^{2\,tstop}$	8
Effective rotor radius R_{rotor}, mm	100.5
Rate distribution of the braking forces ϕ, %	20
Tire radius R_{tire}, mm	380
Surface of the pad A_c [mm^2]	5246
Factor of charge distribution of the disc ε_p	0.5
Surface disc swept by the pad A_d, mm^2	35993

Table 2. Mechanical properties of the disc and pad.

Properties	Disc	Pad
Thermal conductivity, k (W/m°C)	57	5
Specific heat, c (J/kg °C)	460	1000
Thermal expansion, α (10^{-6}/°C)	10.85	10
Young modulus, E (GPa)	138	1
Poisson's ratio, v	0.3	0.25
Density, ρ (kg/m^3)	7250	1400
Coefficient of friction, μ	0.2	0.2
Angular velocity, ω (rd/s)	157.89	
Hydraulic pressure, P (MPa)	1	

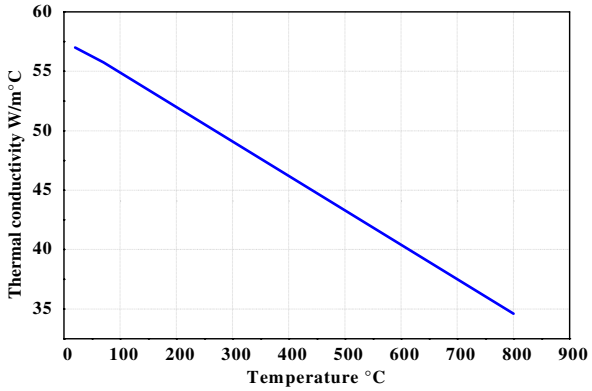

Figure 4. Thermal conductivity vs. temperature.

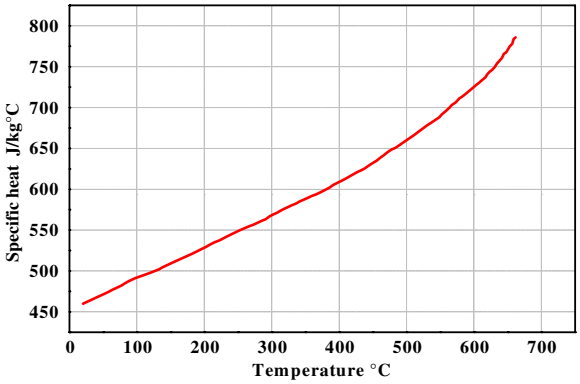

Figure 5. Specific heat vs. temperature.

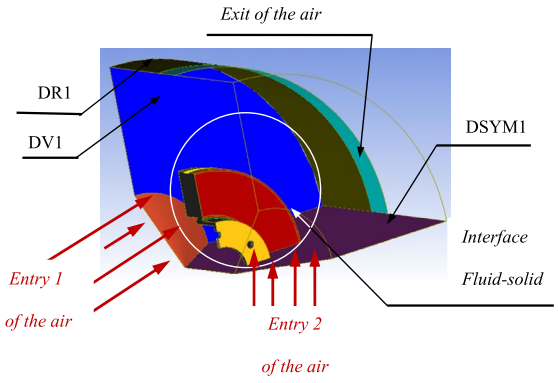

Figure 6. Definition of surfaces of the fluid field.

3.3. Thermal boundary conditions

The boundary conditions are introduced into module ANSYS Workbench [Multiphysics], by choosing the mode of first simulation of the all (permanent or transitory), and by defining the physical properties of materials. These conditions constitute the initial conditions of our simulation. After having fixed these parameters, one introduces a boundary condition associated with each surface.

(1) Total time of simulation = 45 s.
(2) Increment of initial time = 0.25 s.
(3) Increment of minimal initial time = 0.125 s.

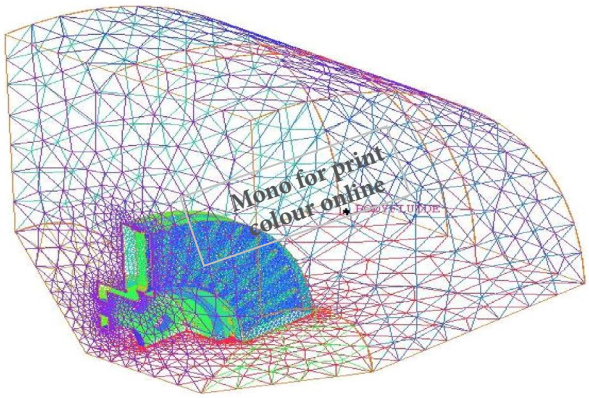

Figure 7. Mesh of the fluid field.

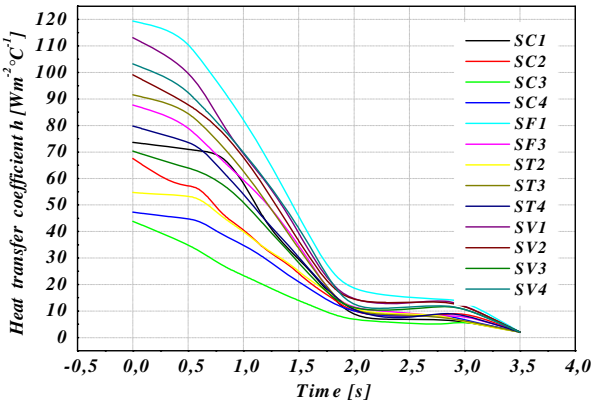

Figure 8. Variation of heat transfer coefficient (*h*) of various surfaces for a full disc in transient case (FG 15).

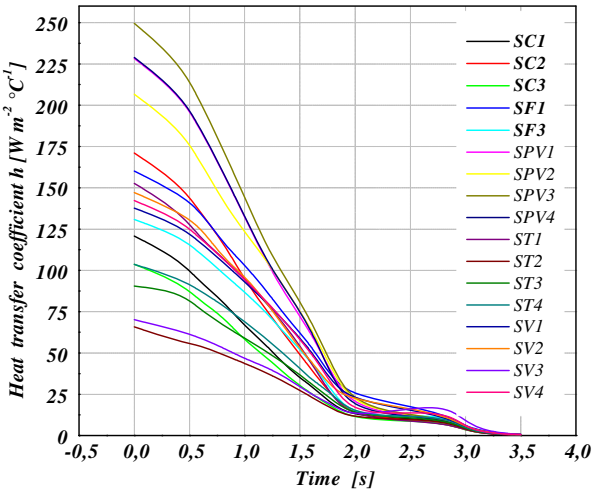

Figure 9. Variation of heat transfer coefficient (*h*) of various surfaces for a ventilated disc in transient case (FG 15).

(4) Increment of maximal initial time = 0.5 s.
(5) Initial temperature of the disc = 20 °C.
(6) Materials: grey cast iron FG 15.
(7) Convection: one introduces the values of the heat transfer coefficient *(h)* obtained for each surface in the shape of a curve (Figures 8 and 9).

Flux: one introduces the values obtained by flux entering by means of the code CFX.

4. FE model and simulation

In this work, a three-dimensional CAD and FE model consists of a ventilated disc and two pads with single slot in the middle as illustrated in Figures 11 and 12, respectively. The materials of the disc and the pads are homogeneous and their properties are invariable with the temperature.

A commercial FE software, namely ANSYS 11 (3D) is fully utilized to simulate structural deformation and contact pressure distributions of the disc brake during single braking stop application. Boundary conditions are imposed on the models (disc–pad) as shown in Figure 13(a) for applied pressure on one side of the pad and Figure 13(b) for applied pressure on both sides of the pad. The disc is rigidly constrained at the bolt holes in all directions except in its rotational direction. Meanwhile, the pad is fixed at the abutment in all degrees of freedom except in the normal direction to allow the pads move up and down and in contact with the disc surface. In this study, it is assumed that 60% of the braking forces are supported by the front brakes (two rotors) as cited in (Mackin et al. 2002). Using vehicle data as given in Table 1 and Equations (1)–(3), braking force on the disc, rotational speed and brake pressure on the pad can be calculated, respectively.

$$F_{\text{disc}} = \frac{(30\%)\frac{1}{2}Mv_0^2}{2\frac{R_{\text{rotor}}}{R_{\text{tire}}}\left(v_0 t_{\text{stop}} - \frac{1}{2}\left\{\frac{v_0}{t_{\text{stop}}}\right\}t_{\text{stop}}^2\right)} = 1047.36[\text{N}] \quad (2)$$

The rotational speed of the disc is calculated as follows:

$$\omega = \frac{v_0}{R_{\text{tire}}} = 157.89 \text{ rad/s} \quad (3)$$

The external pressure between the disc and the pads is calculated by the force applied to the disc; for a flat track, the hydraulic pressure is, as referred to Oder et al. (2009):

$$P = \frac{F_{\text{disc}}}{A_c.\mu} = 1 \text{ [Mpa]} \quad (4)$$

where A_c is the surface of the pad in contact with the disc and μ *is* the coefficient of friction.

5. Coupled thermomechanical analysis

The purpose of the analysis is to predict the temperatures and corresponding thermal stresses in the brake disc when the vehicle is subjected to sudden high speed stops as can occur under autobahn driving conditions. A commercial front disc brake system consists of a rotor that rotates about the axis of a wheel, a caliper–piston assembly where the piston slides inside the caliper, which is mounted to the vehicle suspension system, and a pair of brake pads. When hydraulic pressure is applied, the piston is pushed forward to press the inner pad against the disc and simultaneously the outer pad is pressed by the caliper against the disc. Figure 13(a) shows the FE model and boundary conditions embedded configurations of the model composed of a disc and two pads. The initial temperature of the disc and the pads is 20 °C, and the surface convection condition is applied to all surfaces of the disc and the convection coefficient (h) of 5 W/m^2 °C is applied to the surface of the two pads. The FE mesh is generated using 3D tetrahedral element with 10 nodes (solid 187) for the disc and pads. Overall, 185,901 nodes and 113,367 elements used (Figure 12).

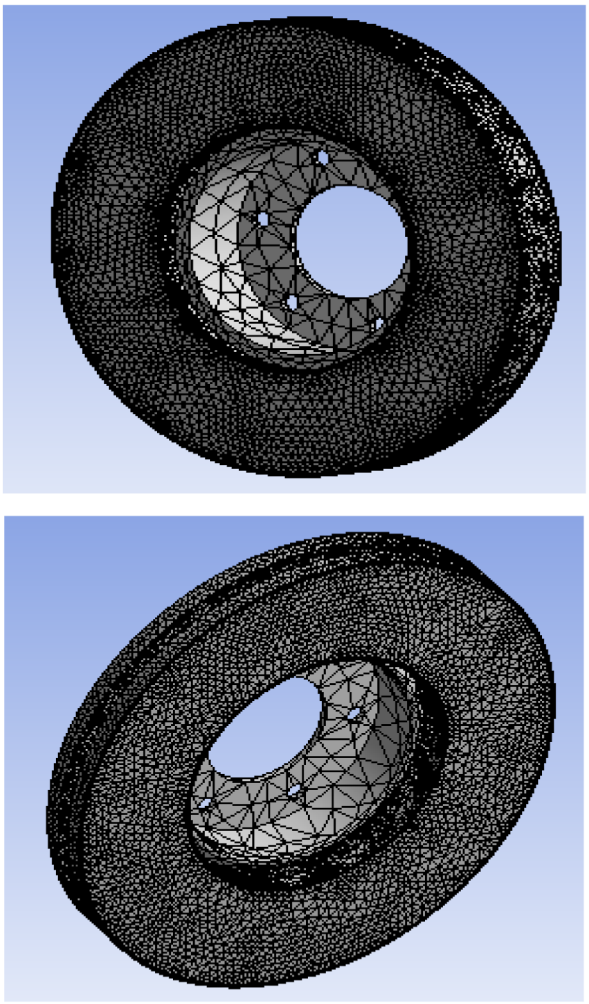

Figure 10. FEA model mesh model for solid disc and ventilated disc.

In this study, a transient thermal analysis will be carried out to investigate the temperature variation across the disc using Ansys software. Further structural analysis will also be carried out by coupling thermal analysis.

6. Results and discussion

6.1. Thermal analysis

Figure 14 shows the variation of the temperature vs. time during the total time simulation of braking for a fall disc and a ventilated disc. The highest temperatures

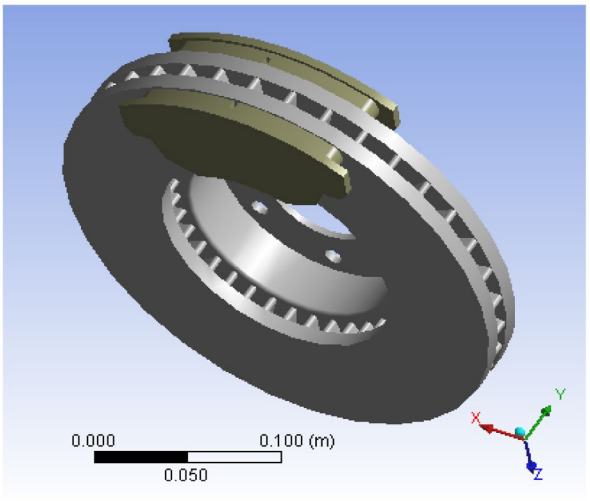

Figure 11. CAD model of the disc and pads.

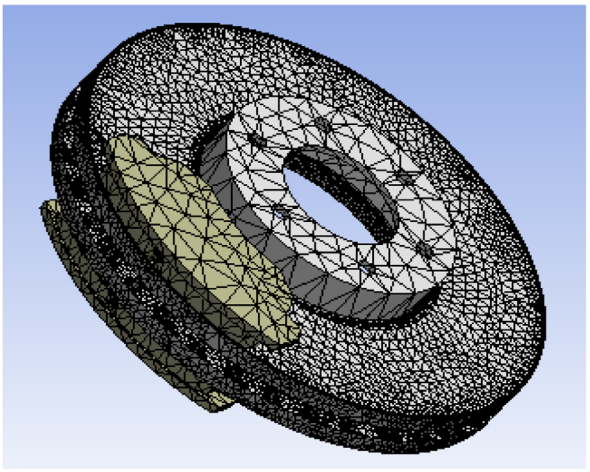

Figure 12. FE model of the disc and pads.

are reached at the contact surface of disc–pads. The strong rise in temperature is due to the short duration of the braking phase and to the speed of the physical phenomenon. For the two types of discs, one disc has an immediate, fast temperature rise followed by a fall in temperature after a certain time of braking.

We can conclude that the geometric design of the disc is an essential factor in the improvement of the cooling process of the discs.

6.2. Von Mises stress distribution

Figure 15 shows distributions of the equivalent Von Mises stress over braking period and it is shown that the highest stress occurs at the bolt holes at the time $t = 0.25$ s. This is due to the disc having experience in torsion and shear modes. This high stress concentration can cause a rupture to the bolt holes.

6.3. Contact pressure distribution

Figure 16 illustrates contact pressure distributions of the inner pad at different braking times. It shows that the contact pressure increases gradually and reaches its maximum value of $P_{max} = 1.8$ MPa at the end of braking period. It is believed that the rise in pressure on the contact surface can also cause a rise in the temperature of the disc and wear of the pads. At the leading side and inner radius of the pad, contact pressure is seen to be higher compared to the other regions. This is due to this area is mostly in contact with the disc surface. Figure 17 shows the evolution of contact pressures along angular positions of the pad. The maximum value of the contact pressure is located at the leading edge and at the level of the lower edge of the pad. Contact pressure distributions of the outer pad are depicted in Figure 18. It shows that the maximum contact pressure is predicted in the middle of the pad with the value of 1.3 MPa. This is much lower than that obtained on the inner pad. Indeed, via a rotating disc brake and in the presence of the centrifugal forces due to the contact disc–pads, it can be product the phenomena of instabilities of the sliding contact in forms of damping following the presence of noise and vibrations phenomena, thus the pressure change at the leading and trailing areas is effected seriously from lining thickness. As the lining thickness, the tilting moment is being increased considerably. Since the pressure increase at the leading side and pressure decrease at the trailing side are symmetrical, the total braking moment won't be changed.

6.4. Effect of a fixed caliper

For a comparative study, the effect of a fixed caliper (disc with double pressure) is also simulated where it maintains the same boundary conditions used in the case of a single-piston caliper. Figure 19 shows the levels of equivalent Von Mises stresses in a section of a disc brake at the end of braking period. Unlike the case of the disc with a single-piston caliper, it is noted that the highest stress appears at the outer side of the fins with the value of 8.3 MPa. This is lower than the stress predicted at the bolt holes with the value of 31.4 MPa for single-piston caliper. It is also found that the stress is well distributed to the disc interface compared with stress predicted in Figure 15.

Table 3. Details of mesh model.

Model	Number of elements	Number of nodes
Full disc	114421	172103
Ventilated disc	94117	154679

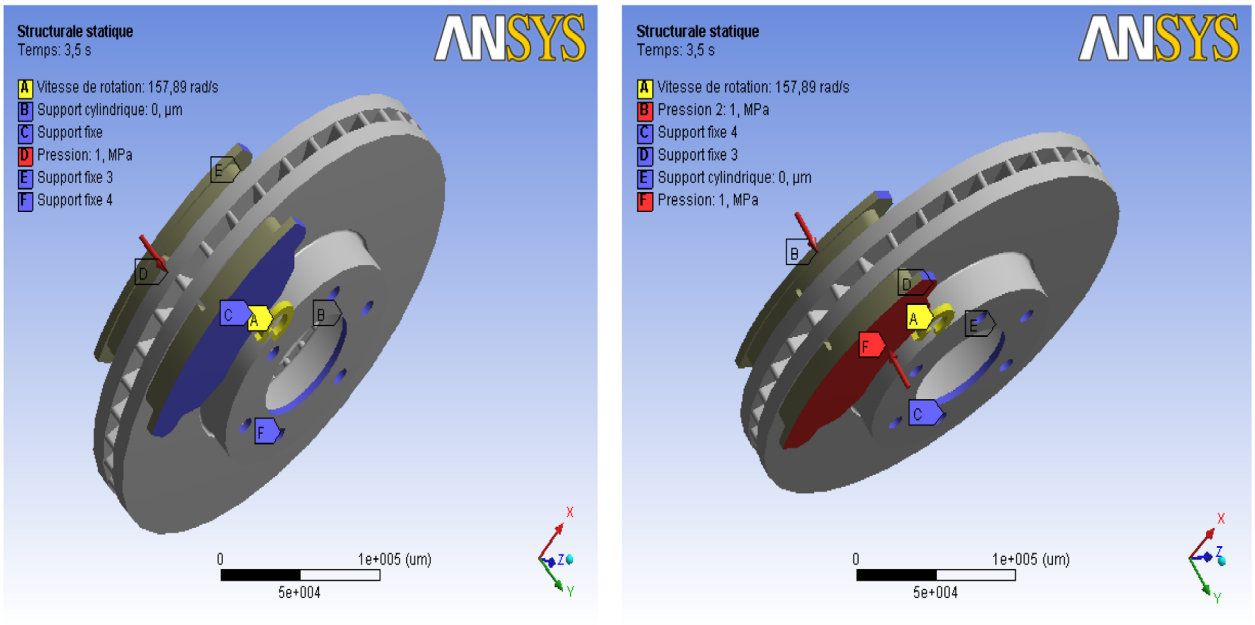

(a) One side (b) Two sides

Figure 13. Boundary conditions and loading imposed on the disc–pads.

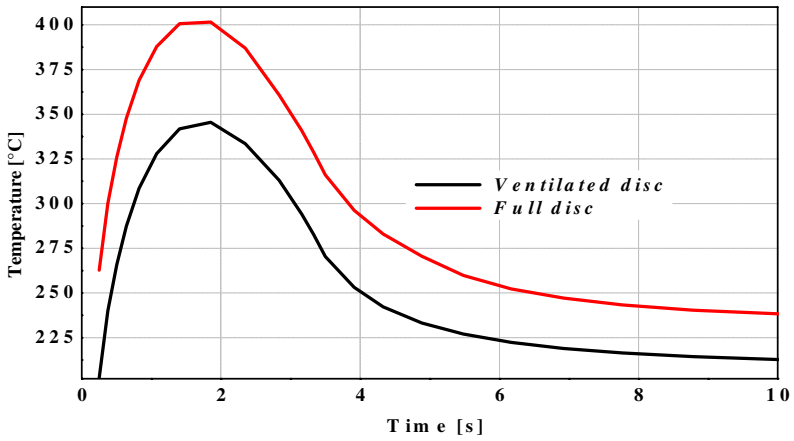

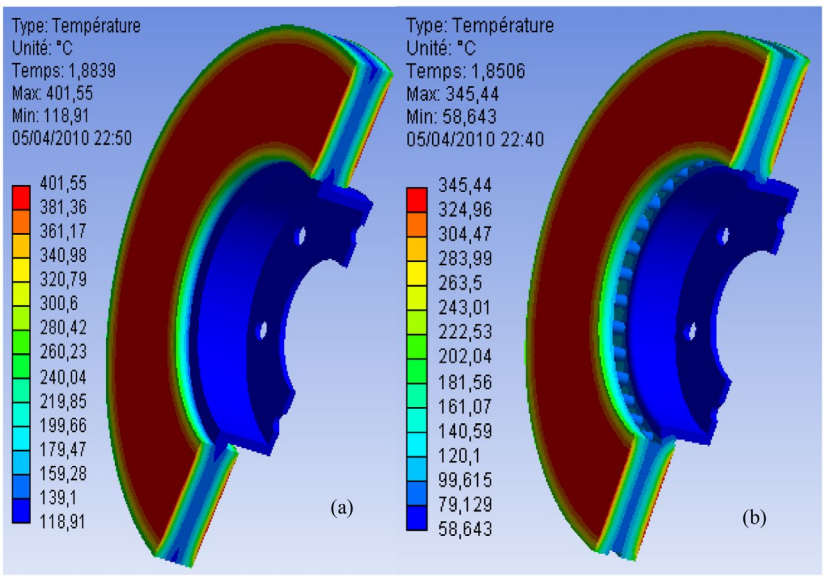

Figure 14. Temperature distribution of a full (a) and ventilated disc (b) of cast iron (FG 15).

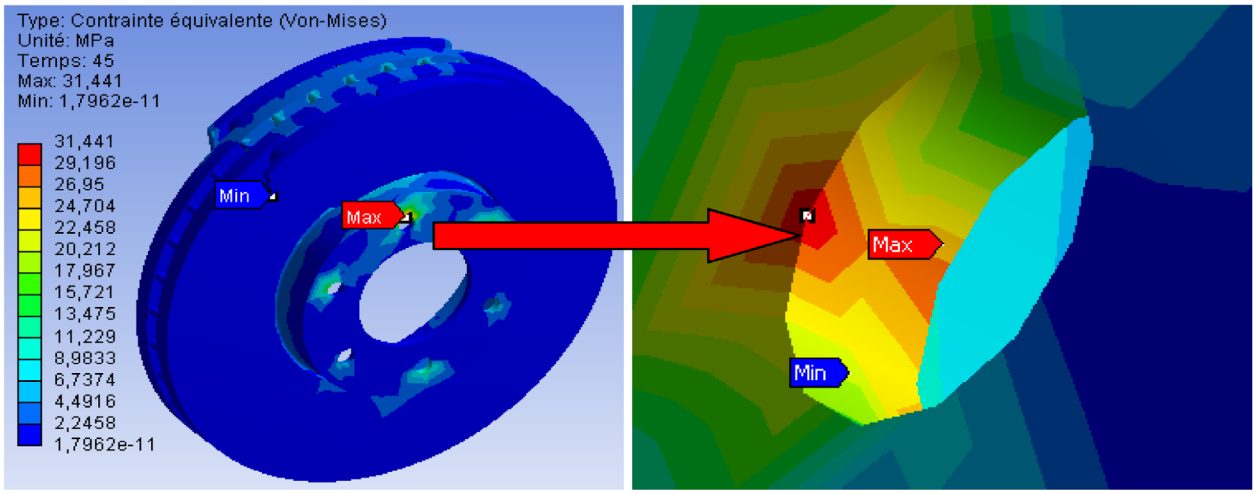

Figure 15. Stress concentration at the bolt holes.

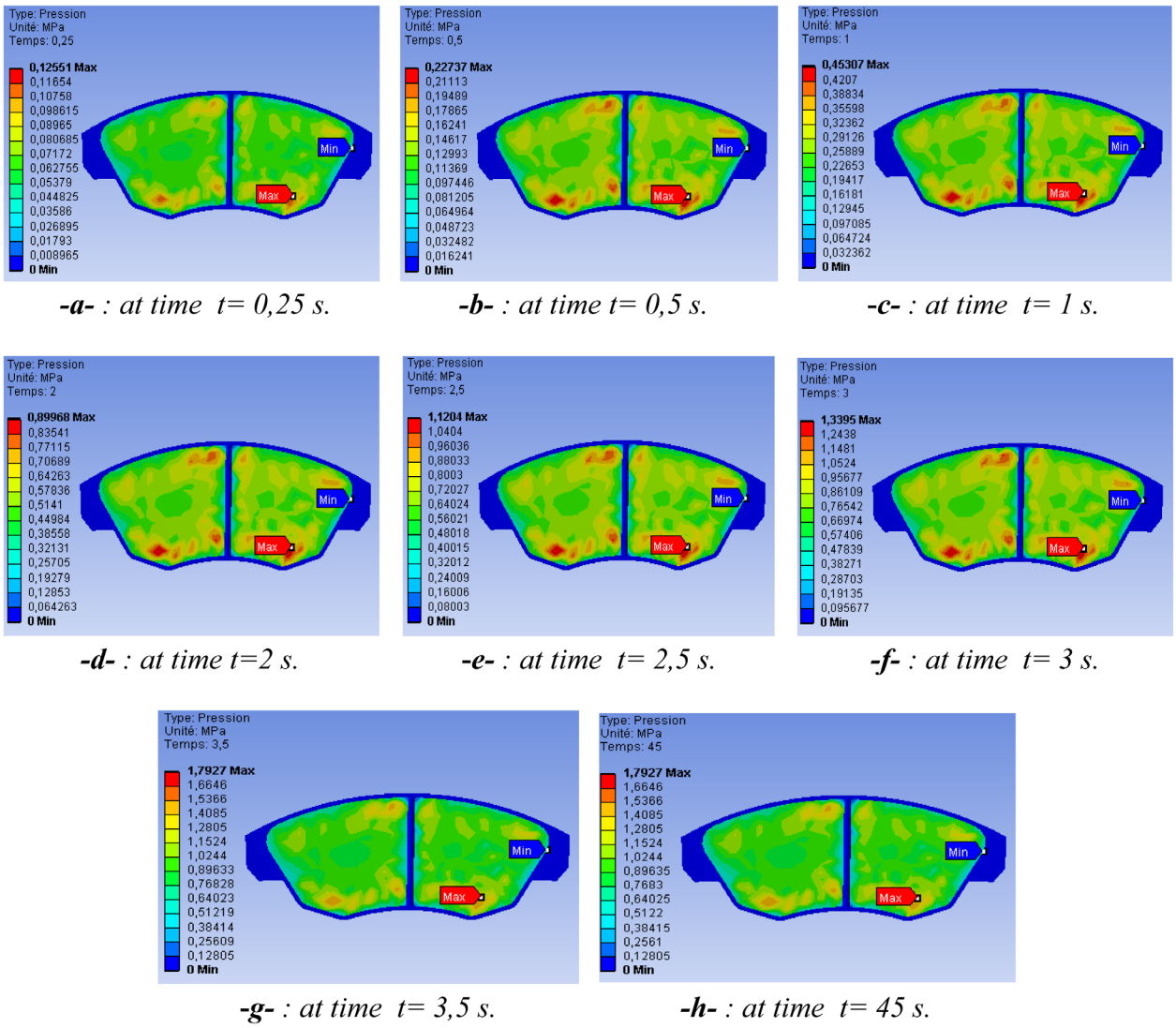

Figure 16. Contact pressure distribution on the inner pad.

6.5. Effect of friction coefficient

It is interesting to see deformation behaviour of the disc and the pads with respect to variation of friction coefficient from 0.25 to 0.35. Figure 20 shows the different configurations of the total deformation of the model in the final stage of braking. It is clearly seen that the total deformation is slightly decreased with an increase in the friction coefficient. Indeed, the high mechanical

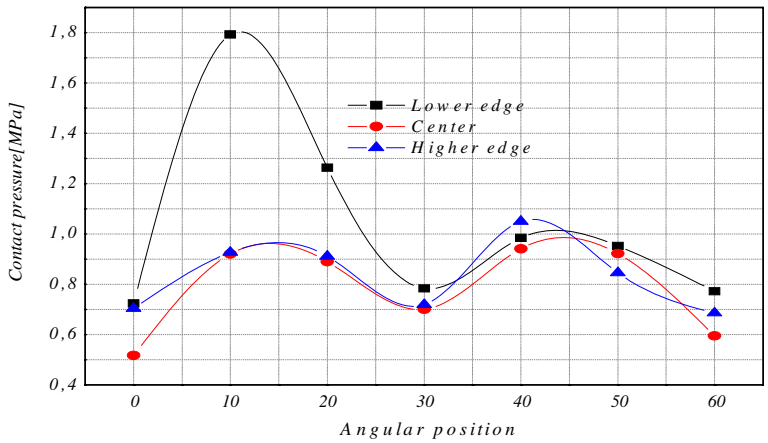

Figure 17. Variation of contact pressures according to the angular position in the inner pad.

advantage of hydraulic and mechanical disc brakes allows a small lever input force at the handlebar to be converted into a large clamp force at the wheel, this large clamp force pinches the rotor with friction material pads and generates brake power. The higher the coefficient of friction for the pad, the more brake power will be generated coefficient of friction can vary depending on the type of material used for the brake rotor. If the value of the coefficient of friction is increased, the disc is slowed down by friction forces which are opposed to its movement, and the maximum deformation that it undergoes is less significant.

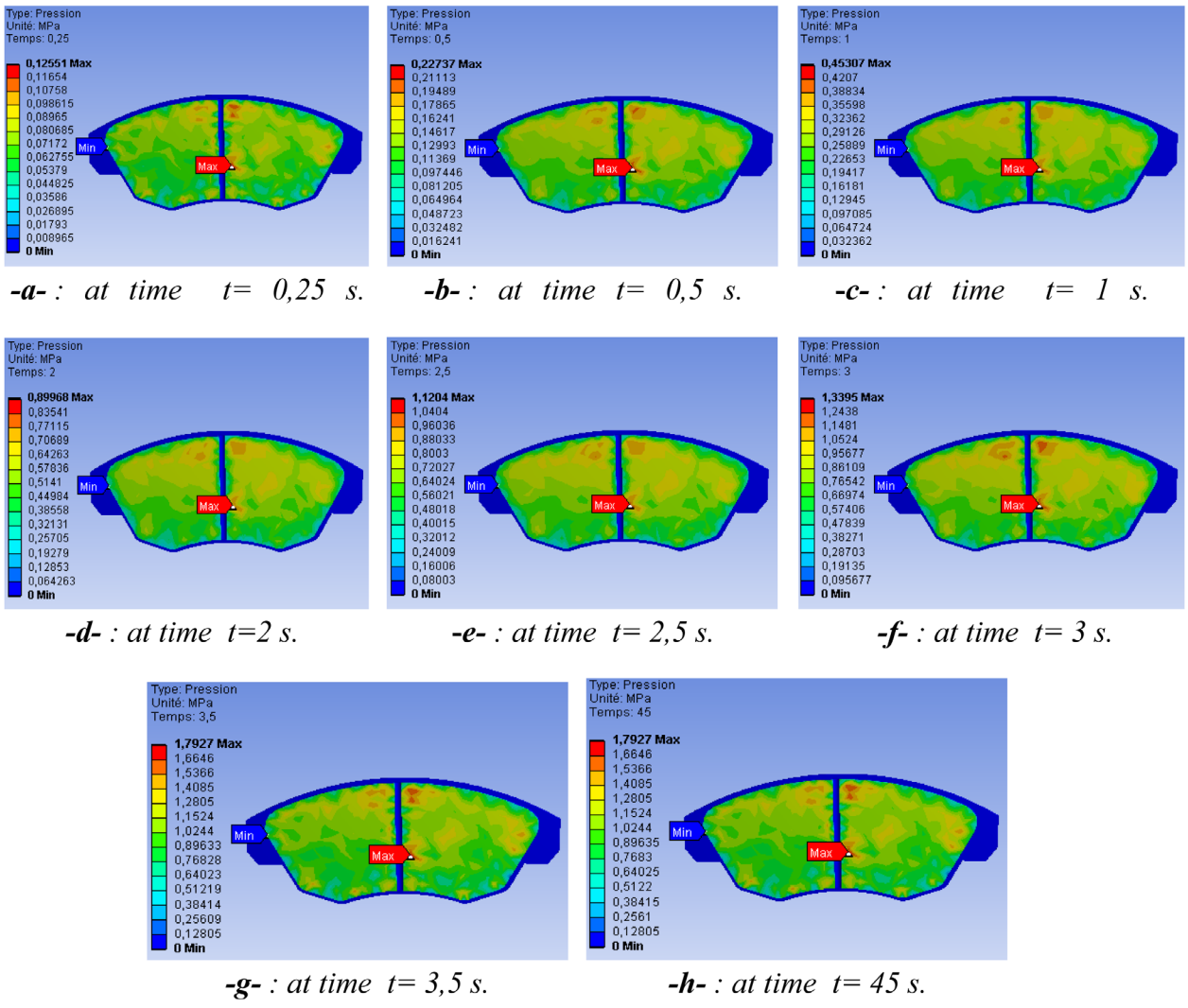

Figure 18. Contact pressure distribution on the outer pad.

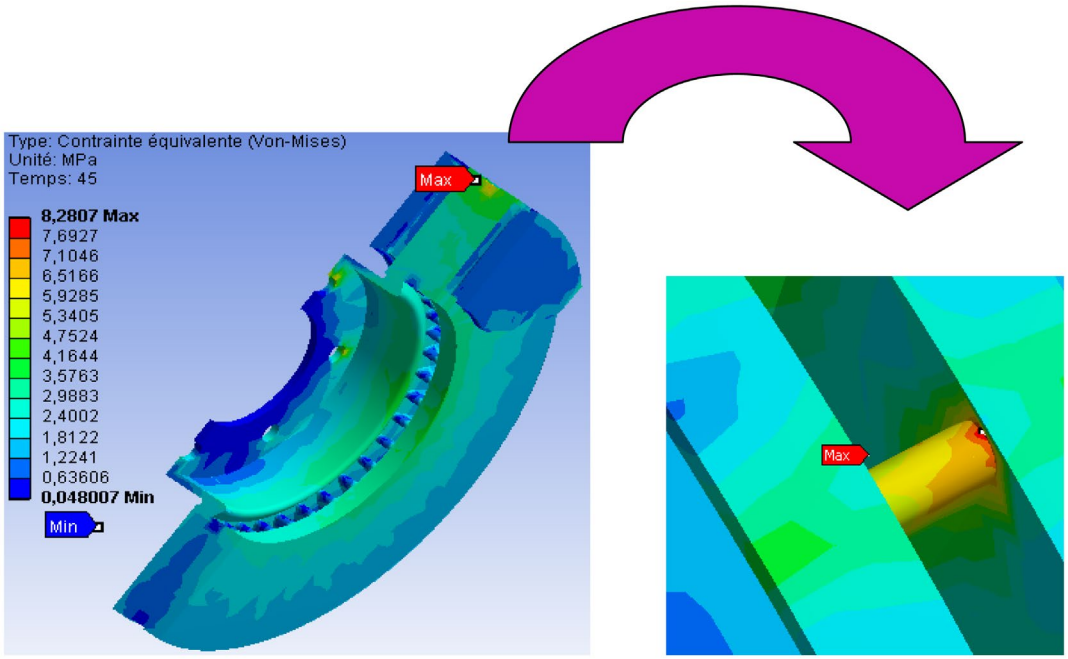

Figure 19. Von Mises stresses.

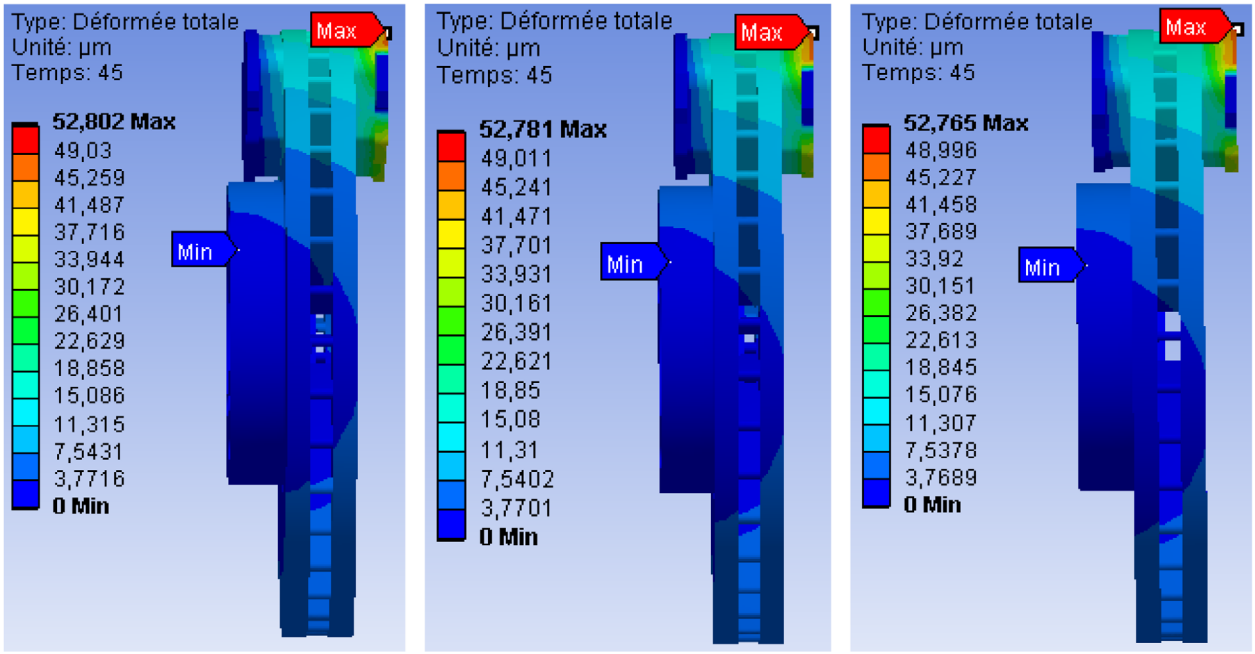

***-a-* : μ =0,25** **-b- : μ =0,30** **-c- : μ =0,35**

Figure 20. Total deformation at the end of braking period.

6.6. *Effect of disc speed*

Figure 21 shows prediction of contact pressure distributions at three different speeds of the disc. It is found that contact pressure distribution is almost identical in all three cases and its value increases with an increase in the angular velocity of the disc. This was also confirmed by Abu Bakar, Ouyang, and Cao (2003). It is believed that this increase can create the wear of the pads as they can leave deposits on the disc, giving rise to what is called "the third body". It is noted that the maximum contact pressure is produced on the pad at the leading edge.

6.7. *Thermal deformation in the coupling field*

Figure 22 gives the distribution of the total distortion in the whole (disc–pads) for various moments of simulation. For this figure, the scale of values of the deformation varies from 0 to 284 µm. The value of the maximum displacement recorded during this simulation is at the moment, t = 3.5 s, which corresponds to

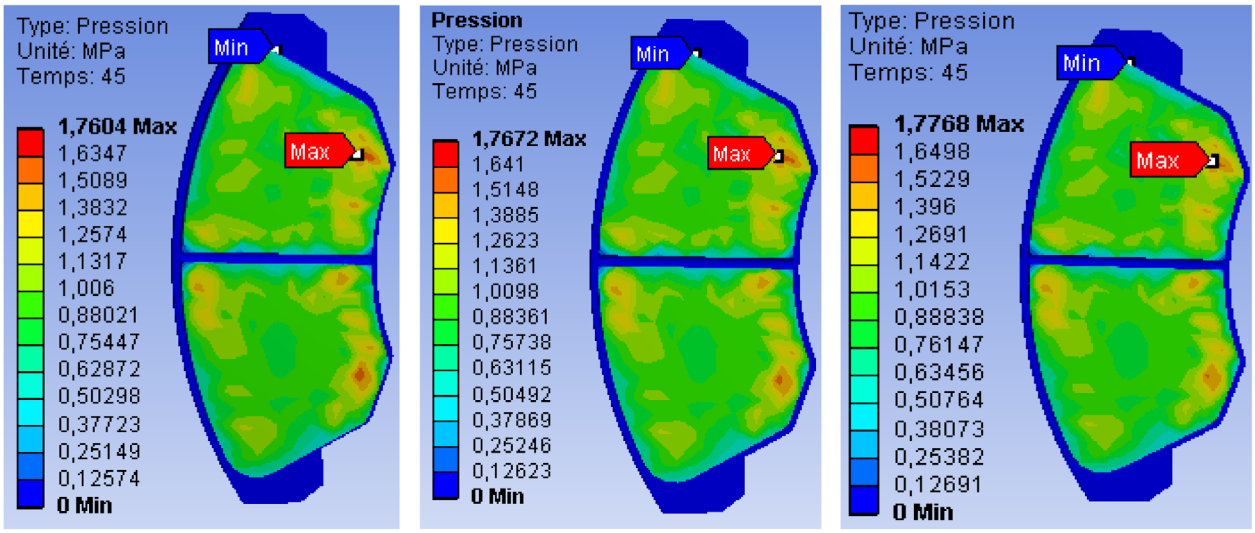

-a- : ω =60 rad/s *-b- : ω =90 rad/s* *-c- : ω =120 rad/s*

Figure 21. Contact pressure distributions.

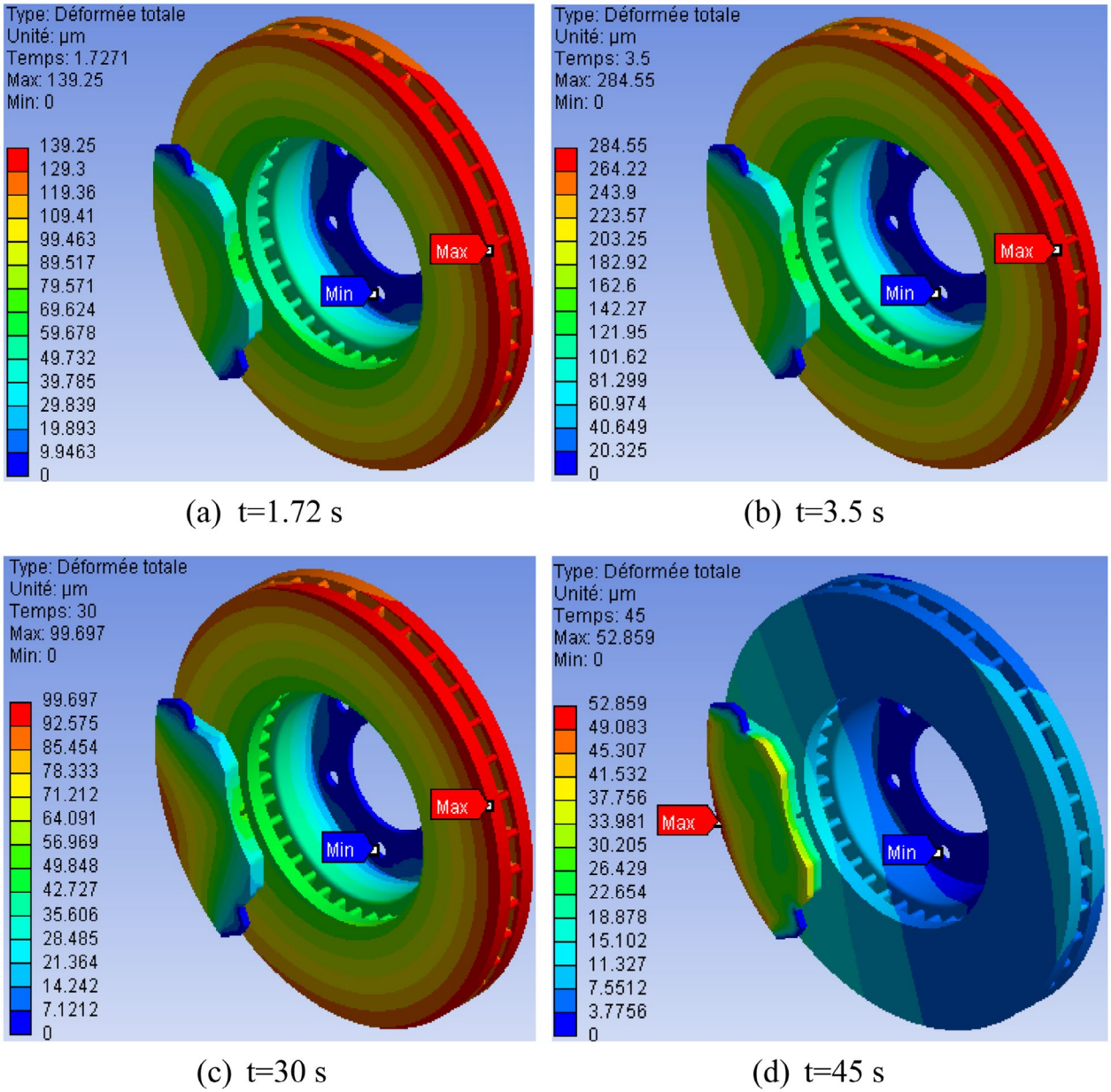

(a) t=1.72 s (b) t=3.5 s

(c) t=30 s (d) t=45 s

Figure 22. Total distortion distribution.

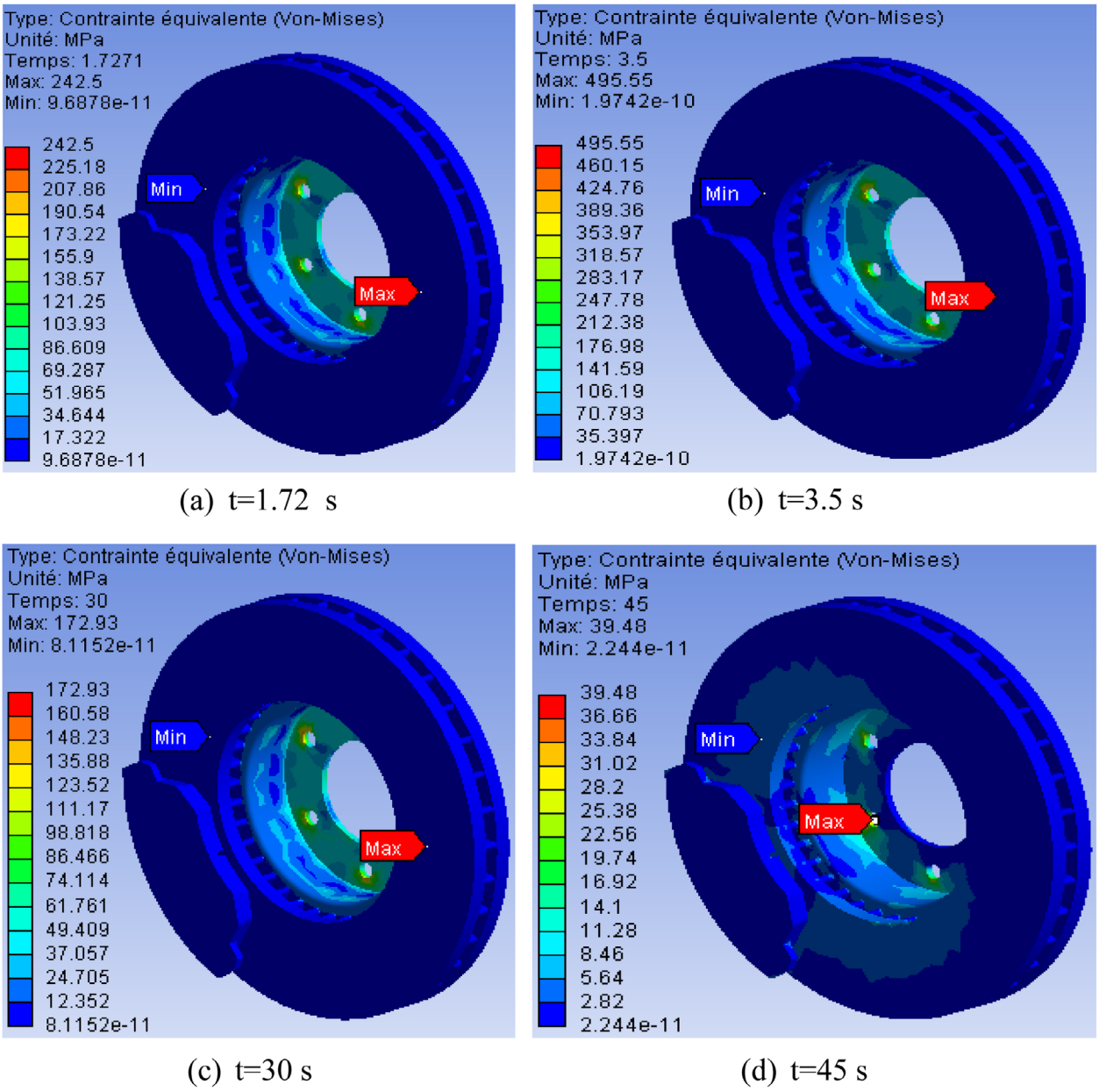

Figure 23. Von Mises stress distribution.

the time of braking. One observes a strong distribution which increases with time on the friction tracks, and the external crown and the cooling fins of the disc. Indeed, during a braking moment, the maximum temperature depends almost entirely on the heat storage capacity of the disc (on particular tracks of friction); this deformation will generate a dissymmetry of the disc following the rise in temperature which will cause a deformation in the shape of an umbrella.

6.8. Von Mises stress distributionin in the coupling field

Figure 23 presents the distribution of the constraint equivalent of Von Mises for various moments of simulation; the scale of values varying from 0 to 495 MPa. The maximum value recorded during this simulation of the thermomechanical coupling is very significant than that obtained with the assistance in the mechanical analysis under the same conditions. One observes a strong constraint on the level of the bowl of the disc. Indeed, the disc is fixed to the hub of the wheel by screws, thus preventing its movement. In the presence of the rotation of the disc and the effects of torsional stress and sheers generated at the level of the bowl, stress concentrations are created. The repetition of these requests will lead to risks of rupture on the level of the bowl of the disc.

7. Conclusion

This paper presents thermal-structural and contact analysis of a reduced brake model without considering thermal effects. The analysis is performed using commercial FE software package, ANSYS where the FE model only consists of a disc and two pads. From the single stop braking simulation, it is found that:

(1) It is concluded that ventilated type disc brake is the best for the present application. All the values obtained from the analysis are less than their allowable values. Hence the brake disc design is safe based on the strength and rigidity criteria.
(2) The bolt holes and outer side of the fins could first damage due to high stress concentration for single and double piston cases, respectively.
(3) Contact pressure is predicted higher at the leading side compared to the trailing side and its value slightly increases with an increase in the disc rotation speeds.
(4) There is no significant change in disc–pad deformation with respect to the variation of friction coefficient.
(5) The total stresss and deformations in the disc increase in a notable way when the system is in thermomechanical coupling.

Regarding the calculation results, we can say that they are satisfactorily in agreement with those commonly found in the literature investigations. It would be interesting to solve the problem in thermomechanical disc brakes with an experimental study to validate the numerical results, for example, on test benches, in order to demonstrate a good agreement between the model and reality.

Regarding the outlook, there are three recommendations for the expansion of future work related to disc brake that can be done to further understand the effects of thermomechanical contact between the disc and pads, the recommendations are as follows:

(1) Experimental study to verify the accuracy of the numerical model developed.
(2) Tribological and vibratory study of the contact disc– pads;
(3) Study of dry contact sliding under the macroscopic aspect (macroscopic state of the surfaces of the disk and pads).

Nomenclature

M	Vehicle mass, kg
v_0	Initial velocity, m/s
t_{stop} t_{stop}	Time to stop, s
R_{rotor}	Effective rotor radius, m
R_{tire}	Tire radius, m
μ	Friction coefficient disc/pad
F_{disc}	Rotor force, N
A_c	Surface of the braking pad, m^2
P	Surface pressure for a single pad, MPa

Notes on contributors

Ali Belhocine received PhD degrees in mechanical engineering at the University of Science and Technology USTO Oran.

Abd Rahim Abu Bakar received his diploma degree in Mechanical Engineering in 1994 from Universiti Teknologi Malaysia. After then, Eng in mechanical engineering at the same university in 1997. He has obtained his PhD degrees in Mechanical Engineering at the University of Liverppol, UK in 2005. His research interests include Automotive Braking Systems, Finite-Element Method (FEM), Automotive Engineering design, vibration, wear and modal analysis, Brake squeel in Abaqus.

Mostafa Bouchetara is a professor of department of Mechanical Engineering from the University of Science and Technology Science and Oran in Algeria (USTO). He obtained his PhD degrees in automotive engineering from the Polytechnic School in Zwickau, Germany. His research areas include the tribology and contact mechanics, heat transfer, energy saving and pollution of internal combustion engines, the statistical methods of design of experiments and numerical methods in engineering optimization.

References

Abu Bakar A. R., H. Ouyang, and Q. Cao. 2003. "Interface Pressure Distribution through Structural Modifications." SAE Technical Paper, 2003-01-3332.
Abu Bakar, A. R., H. Ouyang, and L. Li. 2009. "A Combined Analysis of Heat Conduction, Contact Pressure and Transient Vibration of a Disc Brake." *International Journal of Vehicle Design* 51 (1–2): 190–206.
Gao, C. H., and X. Z. Lin. 2002. "Transient Temperature Field Analysis of a Brake in a Non-axisymmetric Three Dimensional Model." *Journal of Materials Processing Technology* 129: 513–517.
Hohmann, C., K. Schiffner, K. Oerter, and H. Reese. 1999. "Contact Analysis for Drum Brakes and Disk Brakes using Adina." *Computers and Structures* 72: 185–198.
Lee, S., and T. Yeo. 2000. "Temperature and Coning Analysis of Brake Rotor using an Axisymmetric Finite Element Technique." *Proceedings 4th Korea-Russia International Symposium on Science and Technology* 3: 17–22.
Limpert, R. 1999. *Brake Design and Safety*. 2nd ed. Warrendale, PA: Society of Automotive Engineers.
Mackin, T. T., S. C. Noe, K. J. Ball, B. C. Bedell, D. P. Bim-Merle, M. C. Bingaman, D. M. Bomleny, G. J. Chemlir, D. B. Clayton, and H. A. Evans. 2002. "Thermal Cracking in Disc Brakes." *Engineering Failure Analysis* 9: 63–76.
Oder, G., M. Reibenschuh, T. Lerher, M. Šraml, B. Šamec, and I. Potrč. 2009. "Thermal and Stress Analysis of Brake Discs in Railway Vehicules." *Advanced Engineering* 3 (1): 95–102.
Reimpel J. 1998. *Braking Technology*. Vogel Verlag, Würzburg.
Ripin Z. B. M. 1995. "Analysis of Disc Brake Squeal using the Finite Element Method." PhD thesis, University of Leeds.
Söderberg, A., and S. Andersson. 2009. "Simulation of Wear and Contact Pressure Distribution at the Pad-to-rotor Interface in a Disc Brake using General Purpose Finite Element Analysis Software." *Wear* 267: 2243–2251.
Tamari, J., K. Doi, and T. Tamasho. 2000. "Prediction of Contact Pressure of Disc Brake Pad." *Society of Automotive Engineering, Review* 21: 133–141.
Tirovic, M., and A. J. Day. 1991. "Disc Brake Interface Pressure Distributions." *Proceedings of the Institution of Mechanical Engineers, Part D* 205: 137–146.
Valvano T., and K. Lee. 2000. "An Analytical Method to Predict Thermal Distortion of a Brake Rotor." SAE Technical Paper, 2000-01-0445.
Wolejsza, Z., A. Dacko, T. Zawistowki, and J. Osinski. 2001. "Thermo-mechanical Analysis of Airplane Carbon-carbon Composite Brakes using MSC." Marc, Warsaw University of Technology, Paper 2001-58.